

# Influence of Interface Modification and Phase Separation on Damping Properties of Epoxy Concrete

Shiqun Li, Jiashan Hu, Fangzhen Song & Xiaoxuan Wang

Department of Materials and Engineering, Shandong Building Materials Institute, Jinan, Shandong, China

(Received 28 February 1996; accepted 9 September 1996)

## Abstract

*A preliminary study has been conducted to investigate the influences of interface modification and rubber phase separation on damping behaviour of epoxy concrete (EPC). The main parameters studied here are loss factor ( $\eta$ ), i.e. damping, and dynamical modulus of elasticity ( $E_d$ ). It is found that the tenacity of EPC can be improved by controlling rubber phase separation, and that the mechanical vibration can be absorbed while keeping a high enough  $E_d$  value by forming an elastic interlayer using a coupling agent and acrylonitrile-butadiene rubber with end carboxyl group. The values of  $\eta$  and  $E_d$  obtained in this paper are in the range of 0.0436–0.0534 and 20.97–26.72 GPa, respectively. The interface microstructure of EPC has been characterized by means of XPS and FT-IR here. The results suggest that a weak Lewis acid-base reaction has taken place and chemically bonded joints have formed in the interlayer of EPC, and the rubber phase separation has been characterized by the technique of microimage analysis. © 1997 Elsevier Science Limited*

**Keywords:** Epoxy concrete, interface modification, interface microstructure, damping, elastic modulus, rubber phase separation, chemically bonded joints.

## INTRODUCTION

As a new material, polymer concrete (PC) has increasingly more uses because of its many fine properties, among which high damping is very

important for structural materials, such as aviation, navigation, machineries and constructions to absorb the harmful vibration or to minimize the amplitude to a safe level. In 1937, the German navy proposed and studied damping materials first. In the 1960s, Schutz *et al.*<sup>1,2</sup> performed much research on PC, and took it as a kind of damping material for partially replacing steel and cast iron to increase the cutting accuracy of machine tools, and to improve the quality of workpieces. The expected features are:

surface quality: mean peak-to-valley  $< 0.1 \mu\text{m}$   
dimensional accuracy  $< 0.5 \mu\text{m}$   
parallelism  $< 0.3 \text{ mm}$  (measuring length 300 mm)

Although engineers have paid great attention in their designs to the structural damping in recent decades, obviously, the damping property of the material itself cannot be neglected. The influences of materials constituents, especially interface on damping, have been increasingly taken into account. As a matter of fact, modified epoxy concrete (EPC) can be a very good absorbing damping material. Then, how can we modify epoxy resin? What is the relationship between the modified EPC structure, especially the interface structure, and its damping performance of a material? The above research field has hardly been reported till now. Damping and dynamical modulus of elasticity are the most essential properties among all the mechanical ones; they are very important in the final application of a structural material. Damping is very sensitive not only to the morphology in a

multiphase system but also to molecule motions and transformations. So it is of scientific and practical significance to make some explanation for dynamical mechanical performance at the level of micro- and sub-micro-structures, even at the level of molecule and atom, so as to understand more and finally to improve the mechanical properties of EPC.

EXPERIMENTAL PROGRAMME

Materials

The types and properties of epoxy resin, hardener, coupling agent and acrylonitrile-butadiene rubber, and the chemical and physical analysis of aggregate and filler, have been listed in Tables 1–5, respectively.

Testing procedures

Aggregate grading for granite and mix proportions for epoxy resin concrete are shown in Tables 6 and 7, respectively. The surface modification of aggregate and filler is in the way in which the particles of granite and limestone powder were coated with macromolecule layer, which is formed by impregnating the particles into the mixture of titanate coupling agent, acrylonitrile-butadiene rubber with carboxyl

group and epoxy resin for 6 h at 40°C. Then, the aggregate and filler impregnated were mixed with organic materials in a two-direction paddle mixer with the mix proportion in Table 7, and were moulded in sizes of 400 × 50 × 25 mm with a pressure of 10 MPa. Each beam specimen was cured for 2 days at room temperature before being demoulded, and was then cured for 4 h at 60°C, followed by 4 h at 80°C and 2 h at 100°C. Figure 1 shows the schematic diagram for the experimental programme, and Fig. 2 shows the damping test system which has been proved to have adequate precision and reliability.<sup>3</sup>

TEST RESULTS AND DISCUSSIONS

After the thermal treatment designed, the beam specimens were cooled down to room temperature, and were then tested mainly for loss factor ( $\eta$ ), elastic modulus and bending strength, and were then cut into small pieces for the characterization of X-ray photoelectron spectrometry (XPS), microimage analysis and Fourier transform infrared (FT-IR) analysis.

Damping performance of EPC

Table 8 shows the influence of surface modification and rubber on the damping performance of

Table 1. Properties of epoxy resin

Type	Softness point (°C)	Value of epoxy (N/100 g)	Total chlorine (N/100 g)	Colloidal speed (min)
E-51	Liquid state	0.48–0.54	<0.02	4–14

Table 2. Properties of hardener (versamide)

Type	Value of amine	Viscosity (cp, 40°C)	Colour (Fe–Co)
TY-650 (H-4)	200 ± 20	1000–10000	< 15

Table 3. Properties of titanate coupling agent

Type	Decomposition temperature (°C)	Colour	Specific gravity (d)	Diopter ( $\eta$ )
NDZ-401	260	Dark red	0.970–0.983	1.470–1.479

EPC. It can be seen that the loss factor has increased by 68% for specimen No. 9131 added with 20% rubber in comparison to specimen No. 9149 (0% rubber), while the value of  $E_d$  decreases only lightly. Even so, both  $\eta$  and  $E_d$  values are not satisfactory. It was not until the surface treatment had been conducted on inorganic aggregate physically and chemically that the values of  $\eta$  and  $E_d$  were stable and high. Comparing specimen Nos 9185, 9186 and

9153, for instance, after surface modification, the value of loss factor is 3.41 and 2.8 times higher than that before surface modification, respectively, and in the meantime,  $E_d$  is 21.16 and 26.70 GPa, respectively. Figure 3 shows the free damping attenuation curves of EPC, mild steel and cast iron. These results suggest that interface modification will be a key factor for improving the dynamical mechanics parameters,  $\eta$  and  $E_d$ , of EPC. A high adhesion elastic inter-layer formed after modifying might act as a 'stress concentrator' when a material is under the action of mechanical vibration, and might create stress concentration in the elastic inter-layer to cause deformation which would cause cycling in the way of expansion and compression. When compressing, the temperature goes

**Table 4.** Properties of acrylonitrile–butadiene rubber

Viscosity (cp)	Carboxylic acid content (%wt)	Nitrile content (%wt)
40–100	3–5	32–35

**Table 5.** Chemical composition of aggregate and filler (% wt)

Material	Composition					
	$SiO_2$	$Fe_2O_3$	$Al_2O_3$	$CaO$	$MgO$	LOI
Granite*	49.52	9.76	13.98	12.57	12.69	
Limestone**	0.45	0.11	0.74	52.15		45.12

\*Specific gravity of granite is 2.659.

\*\*The particle size of limestone is small than 0.08 mm.

**Table 6.** Aggregate grading for granite (%wt)

Grading	Particle size (mm)				
	5–7	3–5	1.25–3.0	0.15–0.63	0.08–0.15
D	11.1	11.1	44.4	20	13.4
F		66.0		34.0	
G		40.0		60.0	
H			64		36

**Table 7.** Mix proportion for epoxy resin concrete (%wt)

X*	Specimen No.	Aggregate	Filler**	Epoxy resin**	Versamide***	Triethanolamine***	Rubber***
D	9131	100	27	13.00	90.00	15.00	20.00
	9149	100	27	8.90	90.00		
F	9154	100	27	8.00	80.00		
	9189	100	27	4.90	35.00	11.00	40.00
G	9153	100	27	9.00	90.00		
	9173	100	27	5.10	90.00		15.0
	9184	100	27	5.00	34.72	11.50	40.0
	9185	100	27	4.90	35.00	11.00	38.0
	9186	100	27	4.90	35.00	11.00	38.0
H	9155	100	27	8.00	80.00		
	9181	100	27	6.50	26.23	11.13	51.0
	9183	100	27	5.73	34.72	11.50	40.0

\*Aggregate grading.

\*\*By the weight percentage of aggregate.

\*\*\*By the weight percentage of epoxy.

up; when expanding, the temperature goes down. This results in a temperature gradient in the neighboring zone and a thermal conduction loss of mechanical vibration; in this way, the damping performance of EPC improves. On the other hand, when a material is under the action of mechanical stress, this kind of elastic inter-layer can also convey the outer stress borne by

the substrate, so as to withstand deformation and result in high elastic modulus of dynamics and bending strength.

Rubber phase separation in EPC

The phase of acrylonitrile-butadiene rubber with end carboxyl group in epoxy resin must be managed to separate for gaining high loss factor. Using the instrument of mode TAST tlus (German) microimage analyser, the rubber phase separation in EPC studied here could be observed clearly in Fig. 4. Table 9 presents the relationship between the microimage statistical analysis of rubber particles and dynamical performances of EPC. Combining Fig. 4 and Table 9, it can be seen that there is a maximum for the rubber phase nucleation rate and phase separation extent at 80°C. This is reasonable in the light of thermal dynamics and kinetics. It can also be seen that the shape of rubber particles becomes more and more regular and

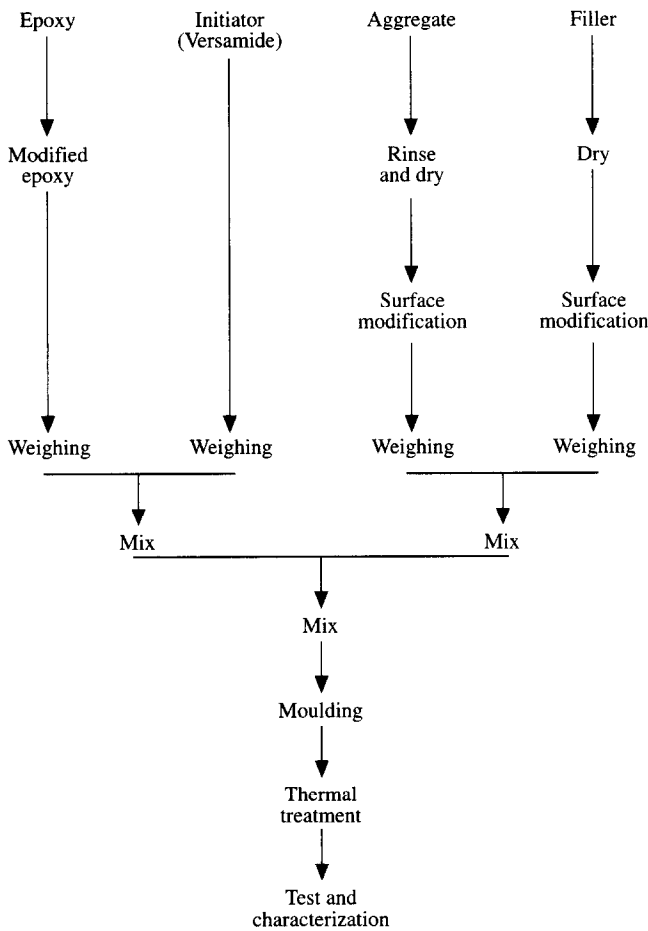


Fig. 1. Schematic diagram for experimental programme.

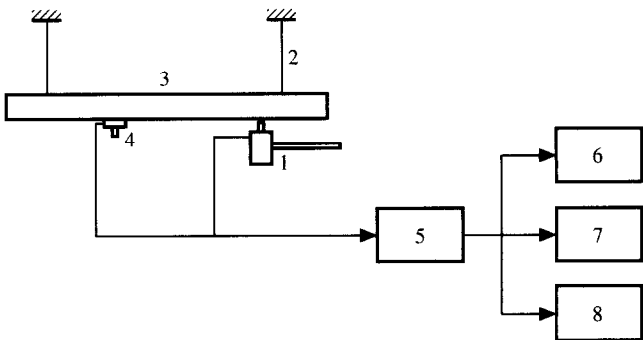


Fig. 2. Instantaneous excitation testing system: 1. hammer; 2. soft supporting; 3. specimen; 4. accelerometer; 5. charge amplifier; 6. signalizer; 7. magnetic tape station; 8. electronic oscillograph.

Table 8. Influence of surface modification and rubber content on damping property

Specimen No.	Surface state*	Rubber**	Loss factor (η)	Elastic modulus (GPa)	Bending strength (MPa)
9131	N	20.00	0.02660	18.25	23.94
9149	N		0.01582	21.87	31.86
9154	N		0.01108	25.48	31.96
9189	Y	40.00	0.04538	20.97	20.35
9153	N		0.01566	21.67	33.24
9173	Y	15.00	0.05080	20.63	
9184	Y	40.00	0.04948	21.82	21.24
9185	Y	38.00	0.05344	21.16	26.15
9186	Y	38.00	0.04364	26.72	26.15
9155	N		0.01060	26.16	36.37
9181	Y	51.00	0.05330	19.36	
9183	Y	40.00	0.04516	22.14	21.29

\*N and Y, indicating the surface of aggregate in specimens has not and has been treated, respectively.  
\*\*By the weight percentage of epoxy.

tends to be a ball with the temperature increasing, and the amount of epoxy resin penetrating into rubber phase reduces, so the boundary becomes more and more clear. Although the optimum temperature for rubber phase separation is  $80^{\circ}\text{C}$ , to take account of both parameters  $\eta$  and  $E_d$  comprehensively, the thermal treatment process of (d) in Fig. 4 has been selected in this study. The phenomenon of rubber phase separation has been proved further by FT-IR in Fig. 5 at wavenumber  $2238$  and  $1731\text{ cm}^{-2}$ , which are character patterns for rubber.

### The relationship of interface structure and damping property

A KRATOS XSAM-800 Surface Analysis System including X-ray photoelectron spectroscopy (XPS) has been applied to study the interface structure of EPC. Each sample was thinned with  $\text{Ar}^+$  ion sputtering in  $4\text{ keV}$  acceleration at the rate of about  $3.5\text{ nm/min}$ , and sample analyses were conducted along the vertical direction, the results being shown in Tables 10 and 11. It can be calculated from Table 10 that

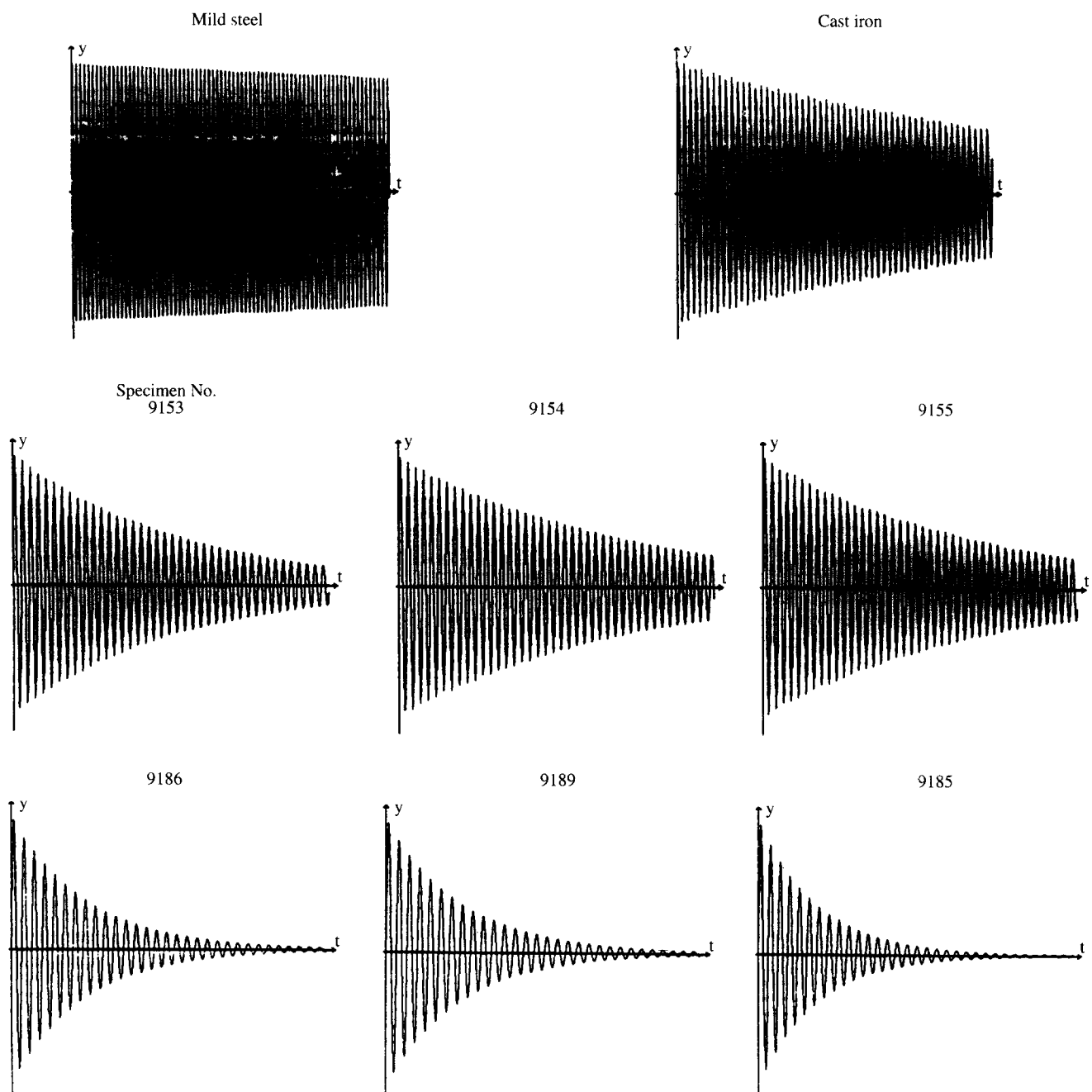
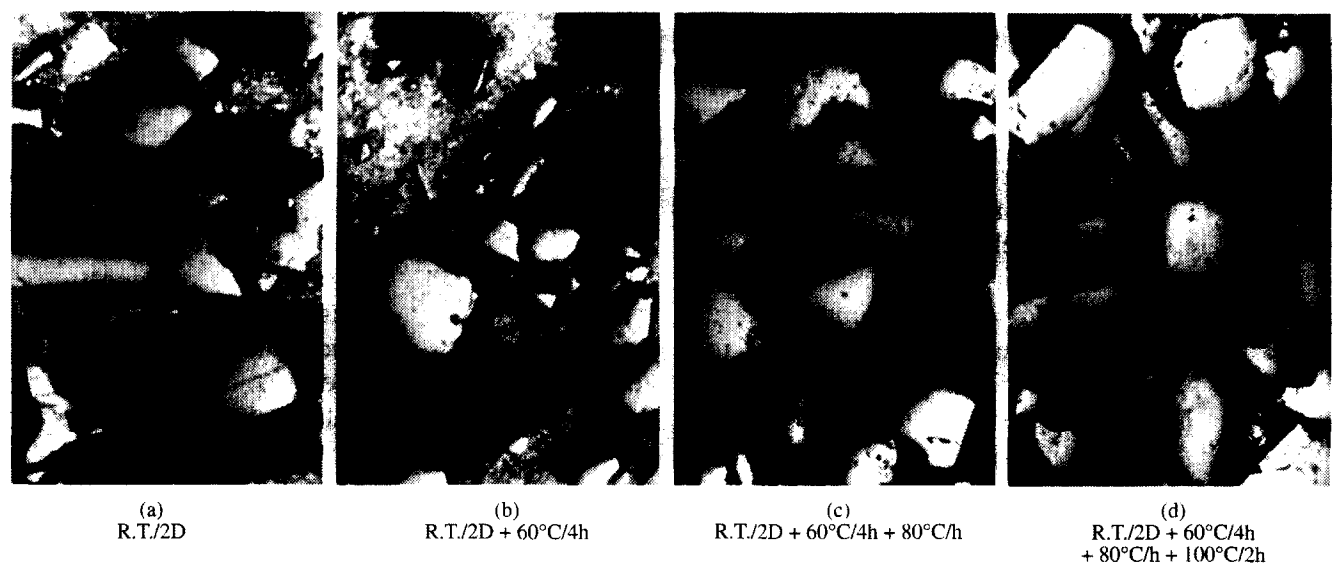


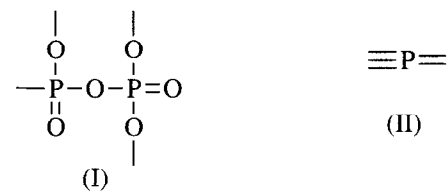
Fig. 3. Free damping attenuation curves for EPC and metals.



**Fig. 4.** Rubber phase separation in modified EPC: (a) RT/2D; (b) RT/2D+60°C/4h; (c) RT/2D+60°C/4h+80°C/h; (d) RT/2D+60°C/4h+80°C/4h+100°C/2h.

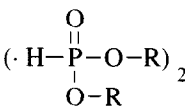
the thickness of the macromolecule coating on aggregate surface is about 25 nm and the results of Table 10 still illustrate that the inter-diffusion of atoms has taken place between polymer and inorganic materials, which creates disorder arrangement of atoms in interface; this might be highly favourable for chemically bonded joints in interface. Table 11 supports this view further. To take the phosphorous atom, for instance, there are two states in its 2p-orbit, and two sub-peaks can be obtained by least square fit, which are in the site of 135.87 and 132.40 eV, respectively, as shown in Fig. 6(b).

These two states of phosphorous atom might be in the forms of (I) and (II) as follows:

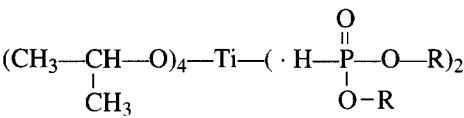


On comparison of the X-ray photoelectron spectrum (a) of P<sub>2P</sub> in surface with that (b) in interface (Fig. 6), the evident change can be

seen. Chemical displacement of bind energy in XPS is caused by charge exchange.<sup>4</sup> The difference of P<sub>2P</sub> electronic bind energy (ΔE<sub>b</sub>) is positive; it indicates that the electronic density in shell decreases, and the shield effect of electron repelling force offsetting against the nuclear attractive force is weakened, which suggests that chemical displacement is caused by electron donation of P<sub>2P</sub>. In the light of the above statement, it can be reasoned that the radical



in titanate coupling agent:



is an electron donor, and present basicity, which might bind with granite (acidity). On the other hand, the difference of Ti<sub>2P3/2</sub> orbit bind energy is negative, radical (O)Ti-R might be taken as electron acceptor, and coordinate with the radi-

**Table 9.** Microimage statistical analysis of rubber particles and dynamic performance of EPC

Sample No.	Temperature (°C)	Mean size of rubber particles (μm)	Number of particles in 1000 μm <sup>2</sup>	Volume percentage × 0.01	Loss factor (v)	Elastic modulus (GPa)
1	RT	28.13	6	0.356	0.1459	12.81
2	60	40.00	9	1.105	0.1212	13.76
3	80	14.00	34	5.257	0.0682	16.77
4	100	12.00	16	1.804	0.0452	22.14
5					0.0428	22.97

cals of  $-N:$  and  $C=O$  in resin until its valence reaches the state of saturation, because the coordination number of ion  $Ti^{+4}$  is less than 6 in titanate coupling agent,<sup>5</sup> hence comes the result that the weak Lewis acid–base reaction has taken place in the interface of EPC. FT-IR spectral analysis, in Fig. 7, supports this. The spectral band shifts and its shape changes markedly in the ranges of  $767\text{--}459\text{ cm}^{-1}$  and  $1731\text{--}1248\text{ cm}^{-1}$ . All the spectral patterns of  $767$ ,  $726$ ,  $668$ ,  $563$  and  $459\text{ cm}^{-1}$  in Fig. 7(b) disappear in Fig. 7(a). The intensity of spectrum  $866\text{ cm}^{-1}$  increases, which might be owing to the bending vibration of radical  $N-H$ . In the range of  $1731\text{--}1248\text{ cm}^{-1}$ , the spectra become

broad which owes much to the stretch vibration of radical  $C=O$  and  $NH_2$  in amide, and to the deformation vibration of  $N-H$ . This change probably motivates to a great extent the ‘crank spin motion’ of several methylene carbon atom chains between amides, hence, this contributes to improve the damping performance of a material.<sup>6</sup> The spectral shape changing might imply much more that some frozen-in chain elements at the interface become able to move and to consume their spare energy in the way of thermal energy, hence, to improve the damping performance of a material. According to the previous discussion, the sketch of interface structure of EPC studied here might be inferred as in Fig. 8.

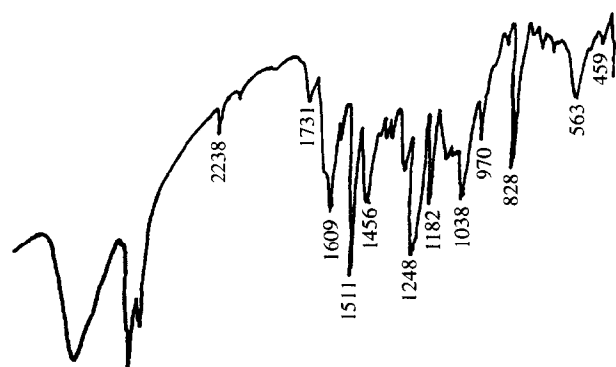


Fig. 5. FT-IR for the comix of epoxy resin and rubber.

## CONCLUSIONS

Advanced dynamics mechanical performances of EPC can be obtained here by means of applying acrylonitrile–butadiene rubber with end carboxyl group to improve the tenacity, controlling rubber phase separation and modifying aggregate surface with macromolecule coating. The dynamic parameters of EPC can be controlled in this study as follows:  $\eta = 0.04362\text{--}0.0534$  and  $E_d = 20.97\text{--}26.72\text{ GPa}$ .

Table 10. Content of main atoms at interfaces of different depths in EPC

Depth (nm)	Content of main atoms (% wt)					
	Atom species					
	Si	Ti	P	N	O	C
0	0	1.39	1.63	6.47	11.7	78.82
7.2	0	7.21	3.28	4.16	17.94	67.93
24.5	0.57	12.05	4.11	3.08	24.60	55.74
59.5	1.07	10.80	2.61	3.07	33.91	48.54
94.5	5.32	9.65	2.41	2.64	40.71	41.54
129.5	28.78	3.86	0	1.81	52.86	12.69
269.5	36.69	0.32	0	0.17	59.26	3.56

Table 11. Bind energy of some atoms at interfaces of EPC

Site	Bind energy of atoms (eV)			
	Electronic orbit			
	$Ti_{2F3/2}$	$P_{2p}$	$Si_{2p}$	$Al_{2p}$
Coupling agent	459.7	133.1		
Aggregate			103.4	73.5
Interface	459.1	135.87	132.40	101.3
Chemical displacement of electronic bind	$\Delta E_b'$	−0.60	+2.77	−0.70
	$\Delta E_b$	−0.60	+2.07	−0.67

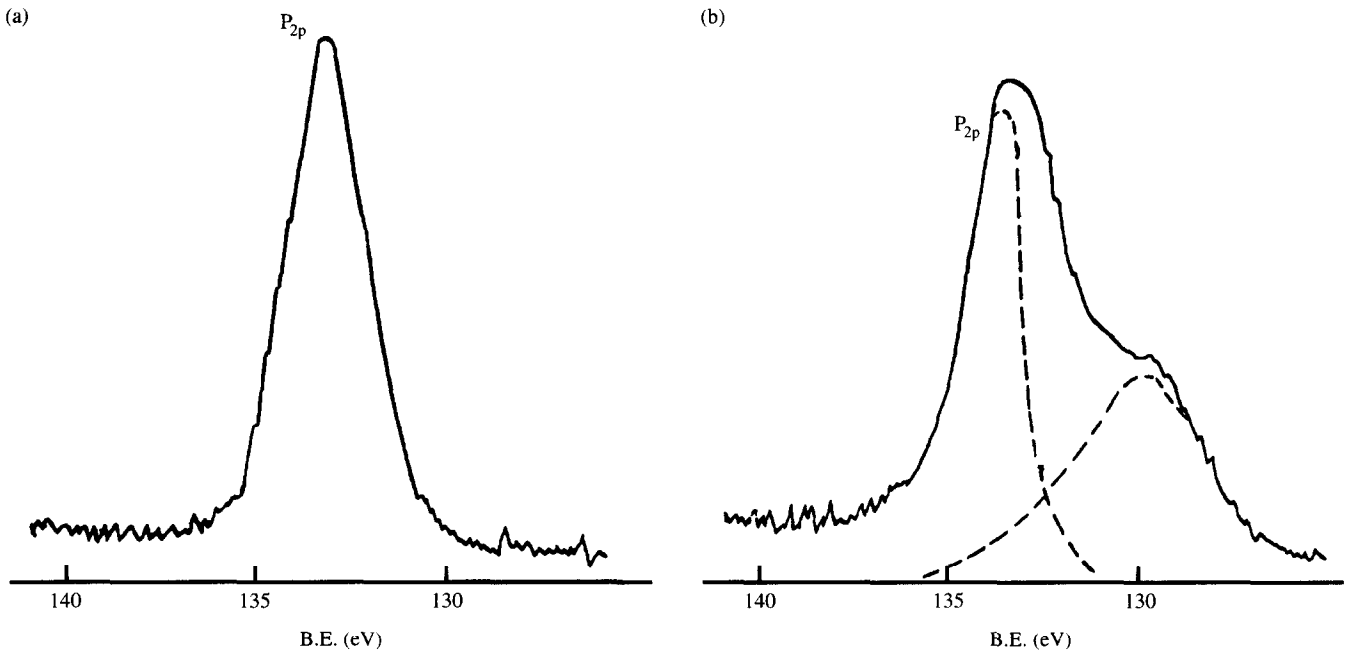


Fig. 6. XPS of phosphorous atom at surface (a) and interface (b).

The improvement of damping ( $\eta$ ) and elastic modulus ( $E_d$ ) of EPC might be owed essentially to the chemically bonded joints in the interface, to the changes of radicals  $C=O$ ,  $N-H$ , at least, to the ‘crank spin motion’ and free vibration of methylene carbon atom chains between amides, and to the formation of elastic interlayer. By

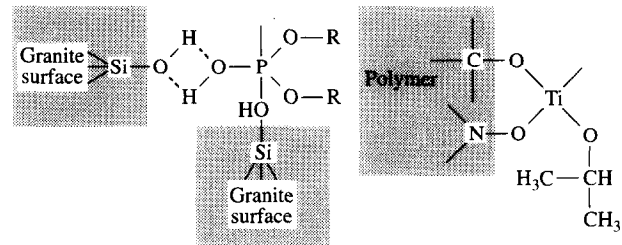


Fig. 8. Sketch of interface structures of EPC.

inference, the interface microstructure of EPC might be drawn as Fig. 8.

ACKNOWLEDGEMENTS

This research has been supported by the Building Materials Development Foundation of The State Administration of Building Materials Industry grant under Contract No. 89-2-07. The authors gratefully acknowledge Prof. Rongxi Shen, the chief engineer of the Institute of Housing Materials and Concrete, China Building Materials Academy, for his valuable advice in this research.

REFERENCES

1. Schutz, H., Statical and dynamical behaviour of machine tool frames made of polymer concrete. *Proc. of 4th ICPIC*, 1984, pp. 121–124.  
2. Tanner, H., Application of polymer concrete in the machine design. *Proceedings of 4th ICPIC*, 1984, pp. 139–144.

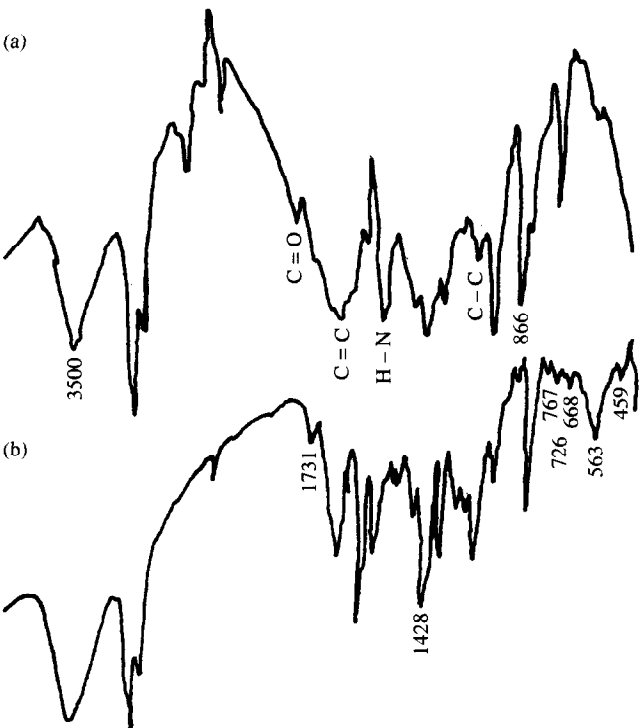


Fig. 7. FT-IR spectra of interface (a) and resin (b) system.

3. Fangzhen S., *et al.*, Measurement and application of dynamic parameters of polymer concrete. *Chinese J. of China Building Materials Science and Technology*, **2**(4) (1993) 17–19.
4. Fowkes, F.M., *Chemistry and Physics of Interface*. American Chemical Society, Washington, DC, 1971, Vol. 2.
5. Longfu Ding *et al.*, Preliminary study on molecular design of titanate coupling agent. *Proc. of 3<sup>rd</sup> National Symposium on Surface and Interface Science of Polymer*, Nanjing University, Nanjing, China, 1990 (in Chinese).
6. Murayama, T., *Dynamic Mechanical Analysis of Polymeric Materials*. Elsevier Science Ltd, The Netherlands, 1978.